Am J Nucl Med Mol Imaging 2017;7(3):138-147
www.ajnmmi.us /ISSN:2160-8407/ajnmmi0057742

Original Article

Multispectral fluorescence guided surgery; a feasibility study in a phantom using a clinical-grade laparoscopic camera system

Danny M van Willigen[1*], Nynke S van den Berg[1,2*], Tessa Buckle[1], Gijs H KleinJan[1,3], James C Hardwick[4], Henk G van der Poel[2], Fijs WB van Leeuwen[1,2]

[1]Interventional Molecular Imaging Laboratory, Department of Radiology, Leiden University Medical Center, Albinusdreef 2, 2300 RC, Leiden, The Netherlands; Departments of [2]Urology, [3]Nuclear Medicine, The Netherlands Cancer Institute-Antoni van Leeuwenhoek Hospital, Plesmanlaan 121, 1066 CX, Amsterdam, The Netherlands; [4]Department of Gastroenterology, Leiden University Medical Center, Albinusdreef 2, 2300 RC, Leiden, The Netherlands. [*]Equal contributors and co-first authors.

Received May 18, 2017; Accepted June 30, 2017; Epub July 15, 2017; Published July 30, 2017

Abstract: Although the possibilities in image guided surgery are advancing rapidly, complex surgical procedures such as nerve sparing prostatectomy still lack precision regarding differentiation between diseased and delicate anatomical structures. Here, the use of complementary fluorescent tracers in combination with a dedicated multispectral fluorescence camera system could support differentiation between healthy and diseased tissue. In this study, we provide proof of concept data indicating how a modified clinical-grade fluorescence laparoscope can be used to sensitively detect white light and three fluorescent dyes (fluorescein, Cy5, and ICG) in a sequential fashion. Following detailed analysis of the system properties and detection capabilities, the potential of laparoscopic three-color multispectral imaging in combination with white light imaging is demonstrated in a phantom set-up for prostate cancer.

Keywords: Imaging systems, prostate cancer, fluorescence, image guided surgery, phantom, laparoscope

Introduction

Due to its ability to visualize disease, fluorescence guidance is increasingly being applied during interventions [1]. The promise of fluorescence imaging to visualize tissue in real-time, possibly with microscopic detail, is considered by many to be a game changer in the manner of performing future surgical procedures. Besides visualizing disease and sentinel lymph nodes, this technology also has the potential to allow differentiation between diseased and healthy tissues (e.g. nerves). Such a differentiation would help to decrease procedure-associated morbidity e.g. long-term functional complications.

Many fluorescent compounds have already found their way into clinical practice, either as a free dye or a dye-functionalized targeting agent [1]. Based on their fluorescence emission spectra, clinically evaluated dyes can be separated into three groups. The first group comprises fluorescent dyes emitting in the visible part of the light spectrum (400-650 nm) with fluorescein being the most widely used visible fluorescence dye in clinical care today. While its routine use lies in angiography, it has also been used successfully to identify ureters [2] and sentinel nodes [3-5]. Moreover, fluorescein in its reactive isothiocyanate form (FITC) can be conjugated to targeting vectors, e.g. NP-41, a peptide developed for the targeting and subsequent visualization of nerves [6, 7]. The second group consists of dyes emitting in the far-red region of the light spectrum (650-750 nm). Here, an interesting development has been the clinical introduction of the relatively bright cyanine dye Cy5. Upon coupling to a c-Met receptor targeting peptide, this dye has proven its value for the visualization of polyps in the colon during colonoscopy [8]. The last group consists of near-infrared emitting cyanine dyes (750-1000 nm) such as indocyanine green (ICG). The clini-

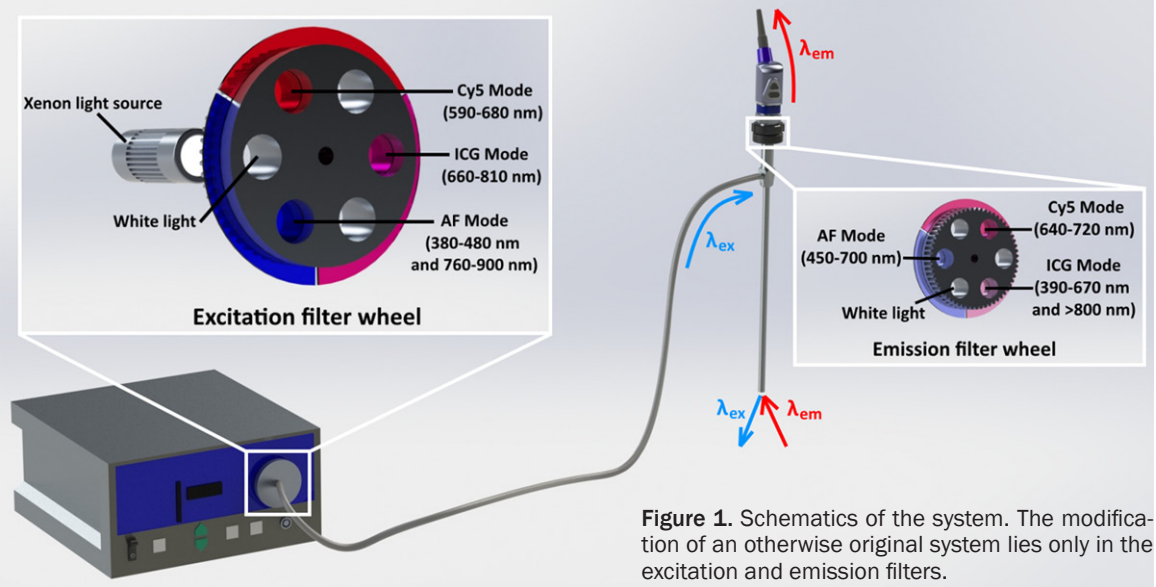

Figure 1. Schematics of the system. The modification of an otherwise original system lies only in the excitation and emission filters.

cal success of the use of ICG in angiography and lymphatic mapping applications [9] has stimulated the development of a wide range of near-infrared fluorescent tracers. Most of these novel dyes (for example 800CW and ZW800) are based on Cy7 analogues that, in contrast to ICG, can also be coupled to a targeting moiety [10].

Multispectral (or multicolor) fluorescence imaging explores the spectral difference between individual fluorescent dyes. Thereby it allows for the concurrent use of multiple fluorescent dyes to highlight various anatomical, physiological and/or molecular features. For this reason, sequential multispectral imaging is routinely being applied in cell biology during analysis of complex cellular effects and in fluorescence immunohistochemistry. In contrast, the use of multispectral imaging approaches *in vivo* can be considered rare. An extraordinary pre-clinical *in vivo* example has been provided by Kobayashi et al., in which they performed lymphatic mapping using five different fluorescent tracers [11]. Only few clinical studies report on the use of multiple fluorescent dyes simultaneously in a single patient. In ophthalmology the near-infrared ICG and visible fluorescein have been used simultaneously to study the vascular physiology of the eye in detail [12]. For sentinel node biopsy procedures in patients with gynecological malignancies, Laios et al. have shown combined imaging of methylene blue (far-red emission) and ICG [13, 14]. Lee et al. demonstrated the combined imaging of fluorescein and ICG for lymphatic mapping during laparoscopic gastrostomy [5]. Our group recently demonstrated that simultaneous use of the hybrid tracer ICG-^{99m}Tc-nanocolloid and fluorescein could provide additional information regarding the location of sentinel nodes during robot-assisted laparoscopic sentinel node biopsy for prostate cancer [15]. Critical for the clinical dissemination of a fluorescence imaging and in particular multispectral image guidance, is the availability of dedicated camera systems capable of detecting the different fluorescent emissions.

For the current study we have generated a prototypical set-up for a clinical fluorescence laparoscope so that it can sequentially detect white light and three non-overlapping fluorescent emissions: visible green (450-650 nm), far-red (650-750 nm) and near-infrared (>750 nm). Subsequently, we characterized the system's performance (looking at a.o. spectral properties, sensitivity and in-depth tissue penetration) using fluorescein, Cy5, and ICG. This was followed by a proof-of-concept evaluation in a clinically-relevant phantom set-up.

Materials and methods

Camera, filters and light sources

For imaging of white light, fluorescein, Cy5 and ICG, a clinical grade IMAGE 1 S camera system

equipped with a 0° laparoscope was used. Three different D-light systems were used as excitation light source: a D-Light C light source (AF/fluorescein), a Cy5-modified D-Light C light source (Cy5), and a prototype D-light P light source (ICG) (all KARL STORZ Endoskope GmbH & Co. KG, Tuttlingen, Germany) where the main variation lies in the filters that were applied in the slots of the filter wheels. The 0° laparoscope had built-in emission filters for fluorescein (autofluorescence (AF) mode) and ICG (ICG mode; Cat no. 26003AGA; KARL STORZ Endoskope GmbH & Co. KG). An additional standard eyepiece adaptor (Cat. No. 20100034 KARL STORZ Endoskope GmbH & Co. KG) was placed in-between the camera and the laparoscope to apply a Cy5 filter as illustrated in the graphical drawing (Solid works Education Edition 2015 SP5.0, Dassault Systémes) in **Figure 1**.

Spectral evaluation of the light sources and emission filters

To record the light spectra of the excitation light sources and respective excitation filters, a Jobin Yvon VS140 linear array fiber spectrometer (Horiba, Kyoto, Japan) in the 310-900 nm range with an integration time of 0.1 ms was used. Note: 310 nm was the lower detection limit of the fiber spectrometer. To improve the signal-to-noise ratio, an average value was calculated for every 19 data points collected. This was done using the "AVERAGE (OFFSET)" formula in Microsoft Excel and resulted in 130 averaged data points. The effect of the emission filters was determined by coupling the same fiber spectrometer to the filtered laparoscopic set-up. This was done at the location were the IMAGE 1 S camera system was otherwise connected via a C-mount coupling. The spectral properties of the emission filters were determined using the non-filtered white-light emission of the respective light source.

Concentration-dependent detection sensitivity of the laparoscopic fluorescence camera system for fluorescein, Cy5 and ICG

To determine the sensitivity of the fluorescence camera for fluorescein, Cy5 and ICG, a 5 mg/mL solution of the dyes was prepared and diluted 1:1 in 36 steps down to 0.15 pg/mL. Fluorescein was diluted in 0.4 M $NaHCO_3$ pH = 9, Cy5 in H_2O, and ICG in H_2O or human serum albumin (HSA) (Albumaan; Sanquin, Amsterdam, The Netherlands) to achieve optimal fluorescence brightness. From each step of the prepared dilution ranges, 100 mL was pipetted in a black 96-wells plate (Cellstar, Greiner Bio-One GmbH, Frickenhausen, Germany). The complete dilution range was then evaluated using the fluorescence camera system. Hereby the tip of the laparoscope was positioned perpendicular to the well plate surface at a distance of 10 cm. This allowed capturing the whole dilution range in the field of view of the camera.

To provide a more quantitative read-out, fluorescence measurements of the dilution range were performed using a Perkin Elmer LS-55 (Perkin Elmer, Waltham, Massachusetts, USA) fluorescence spectrophotometer. For fluorescein λ_{ex} = 480 nm and λ_{em} = 530 nm were used. For Cy5, λ_{ex} = 650 nm and λ_{em} = 670 nm were used. For ICG and ICG-HSA, λ_{ex} = 760 nm and λ_{em} = 800 nm were used. Absorption and emission spectra of the different dyes were recorded using an Ultrospec 3000 (Amersham Pharmacia, Piscataway, New Jersey, USA) and a Perkin Elmer LS-55, respectively.

Evaluation of the tissue penetration of fluorescein, Cy5 and ICG using the laparoscopic fluorescence camera system

To determine the in-depth detection sensitivity of the laparoscopic fluorescence camera set-up, a tissue penetration experiment was conducted in a manner similar to as described previously [16-18]. In brief, a capillary was filled with a 50 μM solution of each dye dissolved in phosphate buffered saline (PBS) (fluorescein and Cy5) or HSA (ICG). The capillaries were then placed on a slice of meat with the tip of the laparoscope being positioned 10 cm above the capillary. Hereafter, fluorescence imaging was performed in the AF (fluorescein), Cy5 and ICG mode. After the first imaging session, another slice of meat (thickness of ~1.5 mm) was placed on top of the capillary followed by taking the following images. Slices of meat were stacked on top of the capillary until the respective dye became undetectable (determined by two independent observers).

Human-like torso phantom

To demonstrate how the multispectral approach may be used in a clinical setting, a human-like

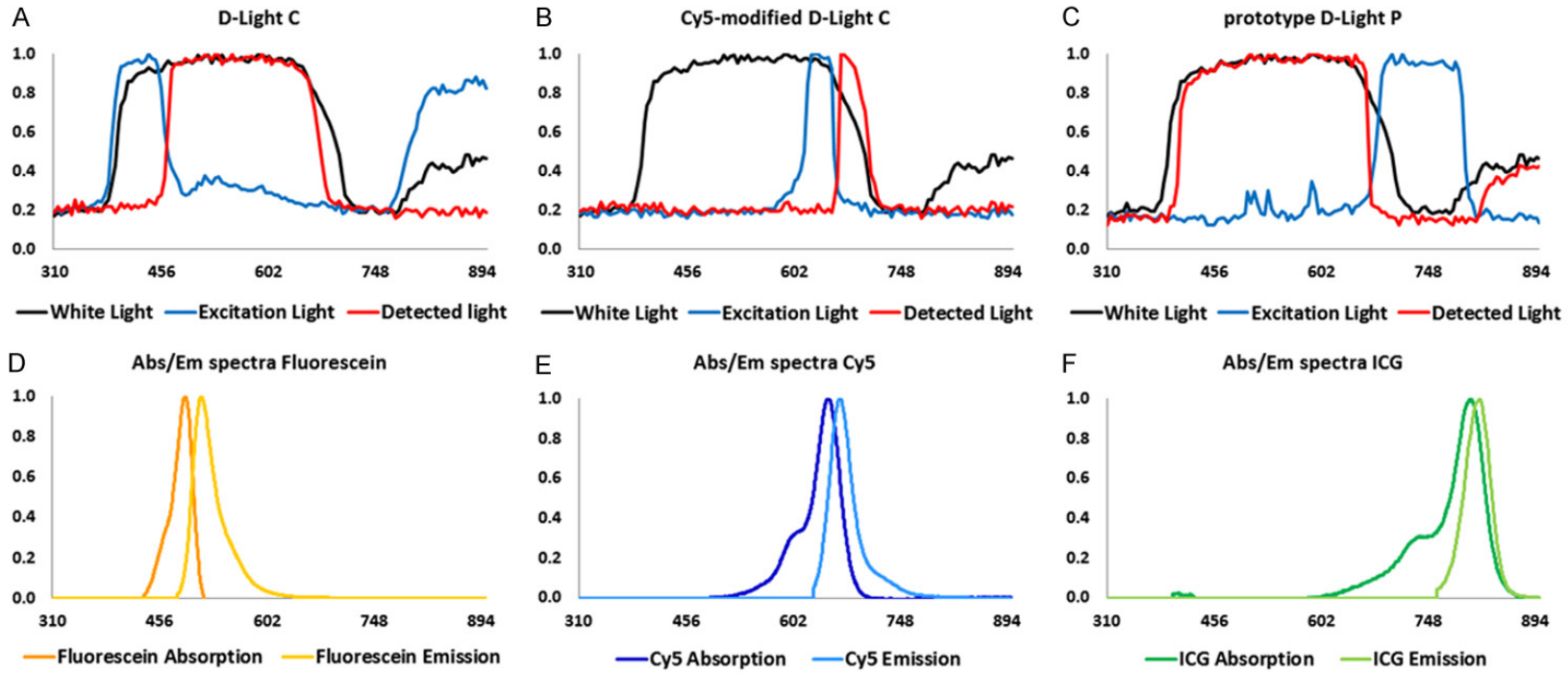

Figure 2. Spectral properties of the laparoscopic set-up in relation to those of the dyes. (A) White light, AF filtered excitation light and detected light from the D-Light C source; (B) White light, Cy5 filtered excitation light and detected light from the Cy5-modified D-Light C source; (C) White light, ICG filtered excitation light and detected light from the prototype D-Light P source; Normalized spectral properties of the dyes (D) Fluorescein (λ_{ex} 483 nm, λ_{em} 512 nm in $NaHCO_3$), (E) Cy5 (λ_{ex} 645 nm, λ_{em} 661 nm in HSA), and (F) ICG (λ_{ex} 807 nm, λ_{em} 818 nm in HSA). Time of irradiation is approximately 10 seconds.

torso phantom was used [19]. With this phantom set-up, a prostate cancer case was mimicked, whereby different fluorescent dyes are used to represent various structures encountered during prostate cancer surgery. In this model, fluorescein-containing lines were used to mimic nerves running through the prostate-related fascia. Three Cy5 beads (two located beneath the surface and one superficial) were inserted into the prostate, thereby representing tumor deposits. Moreover, ICG-containing beads were used to represent sentinel node(s) residing in the pelvic area.

Preparation of the fluorescent beads

To generate Cy5 dye-containing epoxy-resin beads, a 0.1 mg/mL Cy5 in methanol solution was mixed in a volume ratio of 1:100:50 with epoxy resin C and epoxy hardener C (both Faserverbundwerkstoffe GmbH, Waldenbuch, Germany), respectively. For the generation of ICG-containing epoxy-resin beads ICG was dissolved in methanol to a final ICG concentration of 0.1 mg/mL. This solution was then mixed in a in a volume ratio of 1:10:6 ratio with epoxy resin C, and epoxy hardener C, respectively. The resin mixtures were poured in small clay-molds made by pressing an Eppendorf tube (1.5 mL) into molding clay. The resin was allowed to dry for approximately 24 h. Dye concentrations ranged from 0.8 μM to 18.9 μM and were based on their invisibility in white light imaging settings and overlap with the quantities where ICG is commonly detected in the clinic [20].

Preparation of the silicon prostate model

An artificial prostate model was cast from 100 mL Dragon Skin® FX-Pro silicon rubber, 80 mL Slacker® Tactile Mutator (Smooth-On Inc., Macungie, PA, United States) and 300 μL SilTone Fresh Blood pigment (FormX, Amsterdam, The Netherlands). Herein fluorescent Cy5 beads were placed after a small incision.

To generate an artificial fascia around the prostate with nerve structures running through it, again silicon was used. For this 70 mL Dragon Skin® FX-Pro silicone rubber, 70 mL Slacker® Tactile Mutator (Smooth-On Inc.) and 100 μl SilTone yellow pigment (FormX) were mixed. Of this 5 mL was taken and mixed with a fluorescein sodium salt (Sigma Aldrich) stock solution in methanol (1 mg/mL). 75 μL of Thi-Vex® thixotropic agent was added to the remaining 135 mL and after mixing thoroughly this was cast to form a thin covering layer. Immediately after casting, a capillary was used to introduce the fluorescein mixture in the form of intersecting lines. The models were dried overnight.

Results

Excitation and emission spectra

Evaluation of the normalized spectra of the three excitation light sources of which all three had a similar configuration and identical xenon lamp, but differed in the excitation filter applied, showed the excitation light settings in the AF (fluorescein), Cy5 and ICG modes, relative to the non-filtered white light of the xenon lamp which is illustrated in **Figure 2A-C**. These demonstrated excitation filters were specific to the wavelength ranges, 380-480 nm and 760-900 nm (main peaks), 590-680 nm, and 660-810 nm, respectively. To determine the width of the emission filters in the laparoscope, filter settings were studied using white light. As illustrated in **Figure 2A**, light with a wavelength between 450-700 nm was not filtered out in the AF (fluorescein) mode. For Cy5, only light in the 640-720 nm range was allowed to pass through the band-pass filter, as illustrated in **Figure 2B**. In the ICG mode light was only allowed to pass through between 390 nm and 670 nm as well as >800 nm as **Figure 2C** illustrates. **Figure 2D-F** show the matching spectral properties of the fluorescent dyes used, namely fluorescein, Cy5 and ICG.

Sensitivity to the different dyes

To provide insight into how the different fluorescence imaging options of the fluorescence laparoscope relate to the detection sensitivity for the individual dyes, a dilution series of the dyes was generated and measured of which the results are depicted in **Figure 3**. In the well-plate set-up the maximal sensitivity for fluorescein was found to be 0.203 μM. For Cy5 and ICG sensitivities were 0.050 μM and 3.15 μM, respectively. With the laparoscope positioned at a 0.5 cm distance from the surface of the solution the sensitivity improved to 0.051 μM, 0.006 μM and 0.788 μM, respectively. Hereby the limits of visibility were determined by eye and indicated with white circles in **Figure 3B**.

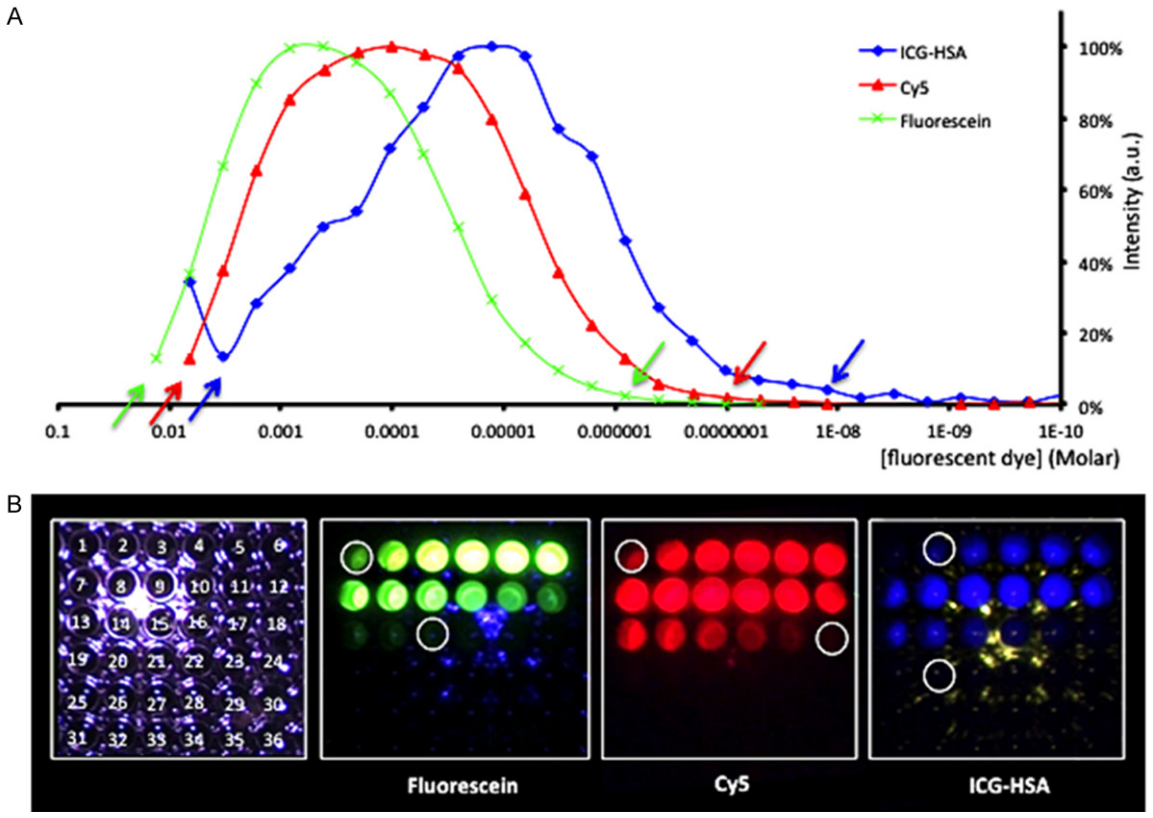

Figure 3. Concentration-dependent detection sensitivity of the laparoscopic fluorescence camera system. (A) Spectral signal intensities determined, and (B) Evaluation of detection limits using the laparoscopic set-up (10 cm; also depicted with arrows in (A). Time of irradiation is approximately 10 seconds. For fluorescein λ_{ex} = 480 nm and λ_{em} = 530 nm were used. For Cy5, λ_{ex} = 650 nm and λ_{em} = 670 nm were used. For ICG-HSA, λ_{ex} = 760 nm and λ_{em} = 800 nm were used.

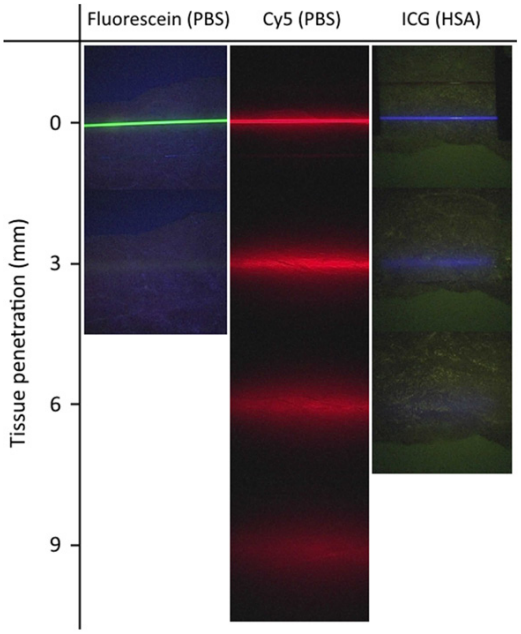

Figure 4. Penetration depth for fluorescein (PBS), Cy5 (PBS) and ICG (200 mg/ml HSA) measured at 10 cm laparoscope distance. Time of irradiation is approximately 10 seconds.

To study the difference in tissue penetration between the different dyes and (fluorescence) imaging settings used, tissue penetration experiments were performed with capillaries containing the individual fluorescent dyes. The difference in penetration depth, which could be visibly assessed on-screen are exemplified in **Figure 4**. The highest tissue penetration was obtained with Cy5 (9 mm). For ICG in HSA a maximum penetration of 6 mm was found, which is in agreement with clinical findings [21]. For fluorescein the tissue penetration was restricted to a mere 3 mm.

Proof of concept three-color multispectral imaging in a phantom set-up

In the human-like prostate cancer phantom, white light and all three fluorescence imaging settings were sequentially applied in the same position as illustrated in **Figure 5**. This experiment illustrated that although different fluorescent emissions are present in the same field of view, the various emission signals could be very easily separated from each other. This became

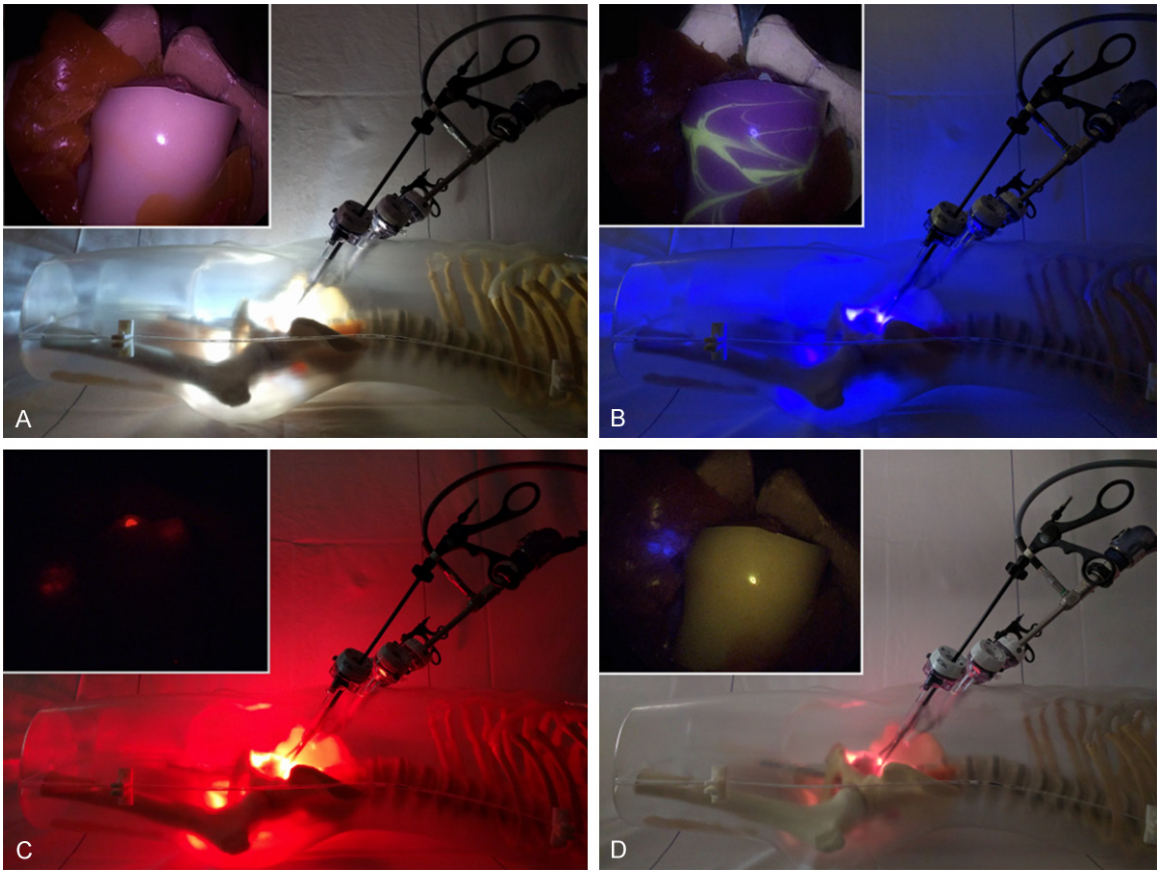

Figure 5. Experimental set-up in a prostate cancer phantom. The outside view of the light source and laparoscopic positioning are shown with the laparoscopic image inserted: (A) White light setting for anatomical context, (B) Autofluorescence setting for the detection of fluorescein (nerves; yellow), (C) Cy5 setting for the detection of Cy5 (tumor lesions; red), and (D) ICG setting for the detection of ICG (sentinel nodes; blue).

most apparent when looking at the fluorescein-containing lines in the silicon that partly overlapped with the location of the Cy5 beads.

Discussion

Previously we demonstrated the feasibility and potential of using two fluorescent dyes, fluorescein and ICG, to provide multispectral fluorescence guidance during prostate cancer surgery [15]. With the current study we show that the laparoscopic camera set-up used in previous clinical trials also allows for imaging of a third fluorescent emission following modification of the excitation and emission light filters [15, 22]. Using this set-up, sequential fluorescence imaging of dyes emitting in the visible to the far-red- and the near-infrared windows has become possible. Where fluorescein and ICG are already routinely used in the clinic, Cy5 will most likely become of great importance for the field in the near future. The chemical freedom to fine-tune Cy5 dye structures makes them a highly suitable fluorescent label for different types of receptor targeting applications [8, 23]. The detection sensitivity of the various dyes studied does not seem to pose limits on the clinical potential to realize a multicolor roadmap towards diseased areas in the body. For all three dyes evaluated, the detection sensitivity was within the detection limits found for ICG in clinical studies [20], namely: 0.006-64.6 μM vs. 0.051 μM, 0.006 μM and 0.788 μM for fluorescein, Cy5 and ICG, respectively. Here the detection sensitivity seems favor Cy5 over fluorescein and ICG.

When assuming an identical photon flux, the penetration depth of a fluorescent dye emitting in the visible or far-red part of the light spectrum (e.g. fluorescein and Cy5, respectively) is less when compared to the penetration depth

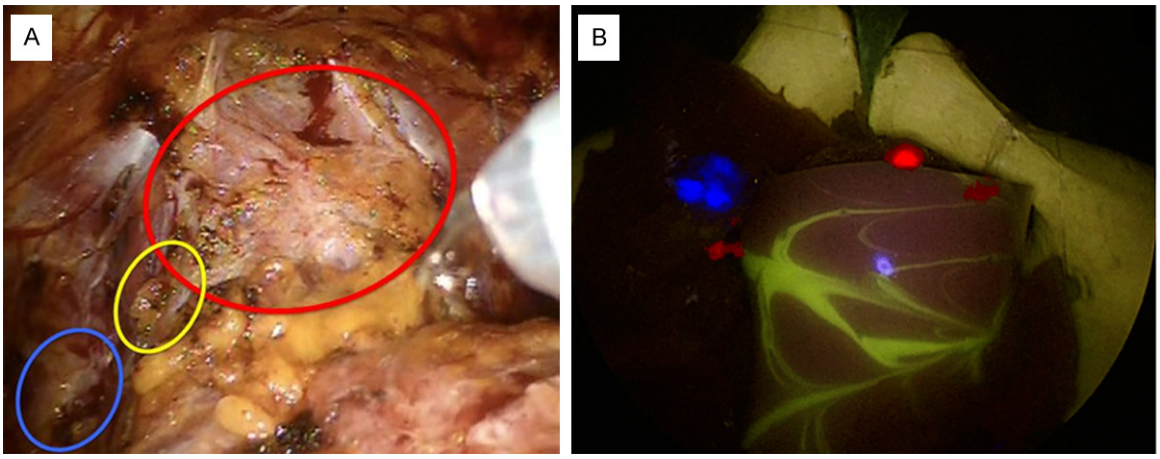

Figure 6. A: Clinical example of the different structures encountered during prostate cancer surgery; and B: Fused multispectral image by manual post-processing. Yellow (circle) represents nerves (fluorescein), red (circle) represents tumor lesions (Cy5) and blue (circle) represents sentinel nodes (ICG).

of a dye emitting in the near-infrared window (e.g. ICG [16, 18]). Nevertheless, our phantom studies indicated that while the application of fluorescein remains confined to superficial structures only (<3 mm), Cy5 in-depth detection actually seemed to be better than that of ICG, as visualized in **Figure 4**. The fact that Cy5 performs this well may be related to its superior brightness relative to ICG. This is a direct result of the difference in quantum yield, 28% for Cy5 vs. 0.3% for ICG [24, 25]. It should be mentioned that, as shown in **Figure 4**, using the current laparoscopic set-up for fluorescein and ICG imaging the fluorescence signal was presented with anatomical background information, whereas the fluorescence signal of Cy5 was shown on a black background. This may, in part, also reflect the detection sensitivities recorded.

In the future, white light imaging in combination with three-color multispectral fluorescence imaging may help enhance precision during more complex surgical procedures, e.g. nerve-sparing (partial) prostatectomy performed in combination with sentinel lymph node biopsy. Our preliminary phantom study suggests that a direct color-based differentiation between (healthy) structures that need to be spared and diseased tissue that needs to be resected is technologically feasible. This said, in the current set-up we used three separate light sources (identical light sources equipped with different excitation filters) and an add-on Cy5 emission filter. Obviously, further hardware integration of the multicolor-fluorescence filter settings and straightforward switching between filter settings would be required in a commercial multispectral fluorescence laparoscope set-up. As the light source and laparoscope both contain filter wheels that can easily be adapted, such modifications seem realistic. From a surgeons point of view sequential imaging is the most convenient mode of fluorescence guidance. Hereby white-light provides the standard for the major part of the procedure and the different features depicted by fluorescence imaging are only used when relevant to the surgical process. Another advantage of sequential imaging is that it limits spectral overlap and thus prevents misinterpretation of the images. This said, like in molecular cell biology where sequential microscopic multispectral imaging is standardly applied, a software-generated overview image that integrates the different views could be valuable as roadmap (**Figure 6**). While the investigated fluorescent emissions are in direct relation to clinical trials in which we have been involved [8, 15, 22], applications of this set-up can easily be extended to alternative combinations of tracers with a similar emission, but then pursuing different targets. Such expansions of the multispectral guidance concept are reliant on the number of fluorescent tracers that are available for clinical use. Hence it is expected to reach increasing clinical relevance during the further maturation of the image-guided surgery research field.

Conclusion

By enabling a clinical-grade laparoscopic fluorescence camera to detect three complementary fluorescent dyes, the potential of laparoscopic three-color multispectral imaging in combination with white light imaging could be demonstrated. This finding, combined with the clinical application of tracers that emit visible-, far-red and near-infrared fluorescence, suggest that multispectral fluorescence imaging has future potential in image guided surgery applications.

Acknowledgements

We thank Dutch Cancer Society translational research award (PGF 2009-4344); NWO-STW-VIDI (STW BGT11272); European Research Council under the European Union's Seventh Framework Programme (FP7/2007-2013) (2012-306890). We also thank KARL STORZ Endoskope GmbH & Co. KG for providing the Cy5 light source prototype.

Disclosure of conflict of interest

None.

Address correspondence to: Dr. Fijs WB van Leeuwen, Interventional Molecular Imaging Laboratory, Department of Radiology, Leiden University Medical Center, Albinusdreef 2, 2300, RC, Leiden, The Netherlands. E-mail: f.w.b.van_leeuwen@lumc.nl

References

[1] van Leeuwen FW, Hardwick JC, van Erkel AR. Luminescence-based imaging approaches in the field of interventional molecular imaging. Radiology 2015; 276: 12-29.

[2] Udshmadshuridze NS, Asikuri TO. Intra-operative imaging of the ureter with sodium fluorescein. Z Urol Nephrol 1988; 81: 635-639.

[3] Dan AG, Saha S, Monson KM, Wiese D, Schochet E, Barber KR, Ganatra B, Desai D, Kaushal S. 1% lymphazurin vs 10% fluorescein for sentinel node mapping in colorectal tumors. Arch Surg 2004; 139: 1180-1184.

[4] Doss LL, Alyea JL, Waggoner CM, Schroeder TT. Fluorescein-aided isolation of lymphatic vessels for lymphangiography. AJR Am J Roentgenol 1980; 134: 603-604.

[5] Lee CM, Park S, Park SH, Jung SW, Choe JW, Sul JY, Yang YJ, Mok YJ, Kim JH. Sentinel node mapping using a fluorescent dye and visible light during endoscopic gastrectomy for early gastric cancer: result of a prospective study from a single institute. Ann Surg 2017; 265: 766-773.

[6] Whitney MA, Crisp JL, Nguyen LT, Friedman B, Gross LA, Steinbach P, Tsien RY, Nguyen QT. Fluorescent peptides highlight peripheral nerves during surgery in mice. Nat Biotechnol 2011; 29: 352-356.

[7] Wu AP, Whitney MA, Crisp JL, Friedman B, Tsien RY, Nguyen QT. Improved facial nerve identification with novel fluorescently labeled probe. Laryngoscope 2011; 121: 805-810.

[8] Burggraaf J, Kamerling IM, Gordon PB, Schrier L, de Kam ML, Kales AJ, Bendiksen R, Indrevoll B, Bjerke RM, Moestue SA, Yazdanfar S, Langers AM, Swaerd-Nordmo M, Torheim G, Warren MV, Morreau H, Voorneveld PW, Buckle T, van Leeuwen FW, Ødegårdstuen LI, Dalsgaard GT, Healey A, Hardwick JC. Detection of colorectal polyps in humans using an intravenously administered fluorescent peptide targeted against c-Met. Nat Med 2015; 21: 955-961.

[9] Alander JT, Kaartinen I, Laakso A, Pätilä T, Spillmann T, Tuchin VV, Venermo M, Välisuo P. A review of indocyanine green fluorescent imaging in surgery. Int J Biomed Imaging 2012; 2012: 940585.

[10] van der Wal S, Kuil J, Valentijn RPM, and van Leeuwen FW. Synthesis and systematic evaluation of symmetric sulfonated centrally C-C bonded cyanine near-infrared dyes for protein labelling. Dyes Pigm 2016; 132: 7-19.

[11] Kobayashi H, Koyama Y, Barrett T, Hama Y, Regino CA, Shin IS, Jang BS, Le N, Paik CH, Choyke PL, Urano Y. Multimodal nanoprobes for radionuclide and five-color near-infrared optical lymphatic imaging. ACS Nano 2007; 1: 258-264.

[12] Jung CS, Payne JF, Bergstrom CS, Cribbs BE, Yan J, Hubbard GB 3rd, Olsen TW, Yeh S. Multimodality diagnostic imaging in unilateral acute idiopathic maculopathy. Arch Ophthalmol 2012; 130: 50-56.

[13] Laios A, Volpi D, Tullis ID, Woodward M, Kennedy S, Pathiraja PN, Haldar K, Vojnovic B, Ahmed AA. A prospective pilot study of detection of sentinel lymph nodes in gynaecological cancers using a novel near infrared fluorescence imaging system. BMC Res Notes 2015; 8: 608.

[14] Volpi A, Tullisa DC, Laios A, Pathiraj PN, Haldar K, Ahmed AA, Vojnovic B. A novel multiwavelength fluorescence image-guided surgery imaging system. Proc SPIE 2014; 8935.

[15] van den Berg NS, Buckle T, KleinJan GH, van der Poel HG, van Leeuwen FW. Multispectral fluorescence imaging during robot-assisted laparoscopic sentinel node biopsy: a first step

towards a fluorescence-based anatomic roadmap. Eur Urol 2017; 72: 110-117.
[16] Chin PT, Beekman CA, Buckle T, Josephson L, van Leeuwen FW. Multispectral visualization of surgical safety-margins using fluorescent marker seeds. Am J Nucl Med Mol Imaging 2012; 2: 151-162.
[17] Chin PT, Buckle T, Aguirre de Miguel A, Meskers SC, Janssen RA, van Leeuwen FW. Dual-emissive quantum dots for multispectral intraoperative fluorescence imaging. Biomaterials 2010; 31: 6823-6832.
[18] Buckle T, Chin PTK, van den Berg NS, Loo CE, Koops W, Gilhuijs KG, van Leeuwen FW. Tumor bracketing and safety margin estimation using multimodal marker seeds: a proof of concept. J Biomed Opt 2010; 15: 056021.
[19] van Oosterom MN, Engelen MA, van den Berg NS, KleinJan GH, van der Poel HG, Wendler T, van de Velde CJ, Navab N, van Leeuwen FW. Navigation of a robot-integrated fluorescence laparoscope in preoperative SPECT/CT and intraoperative freehand SPECT imaging data: a phantom study. J Biomed Opt 2016; 21: 86008.
[20] KleinJan GH, Bunschoten A, van den Berg NS, Valdés Olmos RA, Klop WM, Horenblas S, van der Poel HG, Wester HJ, van Leeuwen FW. Fluorescence guided surgery and tracer-dose, fact or fiction? Eur J Nucl Med Mol Imaging 2016; 43: 1857-1867.
[21] Polom K, Murawa D, Rho YS, Nowaczyk P, Hunerbein M, Murawa P. Current trends and emerging future of indocyanine green usage in surgery and oncology: a literature review. Cancer 2011; 117: 4812-4822.
[22] KleinJan GH, van den Berg NS, Brouwer OR, de Jong J, Acar C, Wit EM, Vegt E, van der Noort V, Valdés Olmos RA, van Leeuwen FW, van der Poel HG. Optimisation of fluorescence guidance during robot-assisted laparoscopic sentinel node biopsy for prostate cancer. Eur Urol 2014; 66: 991-998.
[23] Bunschoten A, van Willigen DM, Buckle T, van den Berg NS, Welling MM, Spa SJ, Wester HJ, van Leeuwen FW. Tailoring fluorescent dyes to optimize a hybrid RGD-tracer. Bionconjug Chem 2016; 27: 1253-1258.
[24] Benson RC, Kues HA. Fluorescence properties of indocyanine green as related to angiography. Phys Med Biol 1978; 23: 159-163.
[25] Mujumdar RB, Ernst LA, Mujumdar SR, Lewis CJ, Waggoner AS. Cyanine dye labeling reagents: sulfoindocyanine succinimidyl esters. Bioconjug Chem 1993; 4: 105-111.